Applied Surface Science Advances 10 (2022) 100269

Contents lists available at ScienceDirect

Applied Surface Science Advances

journal homepage: www.sciencedirect.com/journal/applied-surface-science-advances

Designing a corrosion resistance system using modified graphene oxide-epoxy microcapsules for enhancing the adhesion strength of the epoxy coatings

D. Priyanka *, D. Nalini

Department of Chemistry, PSGR Krishnammal College for Women, Coimbatore, India

ARTICLE INFO

Keywords:
Organic coatings
Graphene oxide
Urea-formaldehyde
Microcapsules
Anti-corrosion
Adhesion

ABSTRACT

New microencapsulated material with advanced corrosion resistance activity and superior adhesion strength on the steel sample was synthesized by in-situ polymerization. In this process, urea-formaldehyde was used as capsule shell material for encapsulating modified graphene oxide. The formation of microcapsules was effectively evidenced by FT-IR, SEM, and TGA-DSC analyses. Initially, graphene oxide was modified by the adsorption of *Catharanthus roseus* L. (C.R) leaves extract and characterized by FT-IR, SEM, EDX, and DFT studies. GO-C.R and UF-GO-C.R (microcapsules) were separately impregnated into epoxy resin and fabricated on the steel substrates. The anti-corrosion performance of UF-GO-C.R/Epoxy in comparison with neat GO-C.R/Epoxy coated sample was evaluated by electrochemical impedance spectroscopy (EIS) and salt spray test. Results reveal that UF-GO-C.R microcapsules in epoxy matrix showed the protection efficiency of 83.6 % after the immersion period of 7 days in 3.5 % NaCl solution which was relatively higher than those with neat GO-C.R. In addition, the coating loaded with UF-GO-C.R microcapsules showed improvement in the adhesion of epoxy coatings on the steel surface which was evident from the increase in peel strength (290 N) through peel-off adhesion test.

1. Introduction

Corrosion causes severe damages to industrial and economical objects and creates a risk to humankind. This gradual deterioration of metallic supplies, either by chemical or electrochemical means, could not be completely prevented. However, various techniques were developed for minimizing this destruction process and improving the adhesion properties, such as surface treatments (applied coatings [1–4], reactive coatings, bio-film coatings, and anodization), restricted permeability frameworks, and the use of corrosion mitigators. Among these strategies, the application of protective coatings gathers global interest because of its practical construction and ability to provide better protection against corrosion [5–11]. Epoxy coatings (organic) are extensively used because they have superior adhesion power onto any substrates, versatility, elevated durability at all temperatures, and outstanding toughness. Epoxy coating on the metal structures creates a passive barrier between the corrosive media and steel substrate. But, the corrosive agents (Cl^-, O_2, and H_2O) penetrate through the microscopic cracks and cavities and reach the surface coating interface. This results in the deterioration of adhesion bonds and blistering of the coating occurs [12,13]. Interestingly, researchers set forth a new strategy to enhance the adhesion strength and anti-corrosion properties of epoxy composites by the addition of pigments and fillers [14–17]. A wide variety of additives have been introduced to congregate the mentioned intention. Liu et al., [11] aimed to minimize the interfacial defects between iron particles and epoxy composites by investigating the effect of controlled grinding temperatures on the compatibility and dispersibility of iron particles. Jiang et al., [9] elucidated the adhesion and anti-corrosion properties of epoxy coatings decorated with silane agents, such as gamma-aminopropyltrimethoxy silane and bis-1, 2-[triethoxysilyl] ethane. Mert et al., [18] prepared epoxy resin doped with polypyrrole- TiO_2 and evaluated the performance of aluminum material against corrosion inhibition.

Recently, these self-healing microencapsulated materials are proved to have the specific property of bringing back the corroded areas to normal. Microcapsules encapsulated with healing agents act as storage and delivery systems in various fields namely drug delivery, construction, food technology, textile, agriculture, aerospace, etc. Wide nano-additives such as graphene and graphite were used as core materials to improve the corrosion resistivity of epoxy coatings. Unfortunately,

* Corresponding author.
E-mail address: priyankapsgrkcw@gmail.com (D. Priyanka).

https://doi.org/10.1016/j.apsadv.2022.100269
Received 21 December 2021; Received in revised form 8 June 2022; Accepted 10 June 2022
Available online 20 June 2022

due to their strong Van der Waals and π- π interactions [19], high ability to agglomerate, lack of dispersion, hydrophobic surface state, and lower surface area, they encounter many challenges in obtaining the most favorable properties of nanocomposites [15,20,21]. One of the best approaches to enhance the dispersivity of graphene is utilizing graphene oxide (GO). Among the various kinds of carbon materials, GO has paid unique attention due to its large surface area and superior chemical properties. The presence of various oxygenous functionalities, namely hydroxyls, carboxyls, and epoxides on its basal planes, declines the mentioned interactions and makes them favorable for dispersion in polymers. However, because of intrinsic Van der Waals interactions [21–27], it results in poor exfoliation and dispersion in organic polymers. This major obstacle could be prevented by decorating graphene oxide sheets with facile functionalities. Microcapsules with changed graphene oxide were excepted to enhance the physical properties of the epoxy system.

The impact of GO sheets embedded in epoxy coatings on anti-corrosion performance has been extensively studied by researchers. Bahar et al. investigated the effect of covalently functionalized GO with diamine [28], polyisocyanate [29], and aminosilane [30] in epoxy, silane-sol based [31] coatings, and found their better barrier performance against corrosive media. Mo et al., [32] prepared polyurethane-based coatings with reinforced GO sheets and evaluated its improved corrosion resistance property after the addition of GO sheets. Recently, Ramezanzadeh et al., [28] reported GO sheets modified by the wet transfer process with amino functionality. This modification enhanced the passive barrier of organic polymer coatings. Chang et al., [33] decorated the graphene oxide sheets by nano casting and produced the corrosion mitigators with more hydrophobic surfaces. These surfaces increase the contact angle from ~82 to ~ 127^{o} and provide extraordinary corrosion protection. Yu et al., [24] improved the dispersion and corrosion protection activity by fabricating GO sheets with Al_2O_3 in the presence of 3-aminopropyltrimethoxysilane. Li et al., [34] improved the anti-corrosion performance of silane composites by adding silanized graphene oxide. All the above works suggest that including additives onto GO sheets can only improve the passive barrier properties and could not heal the mechanical damages created in the coating structure, which is considered being the main inadequacy of GO-epoxy composites. There is no work reported on the microencapsulation of modified GO sheets with superior adhesion bonds and dynamic corrosion mitigating performance.

In the present study, it was determined to enhance the anti-corrosion property and strengthen the adhesion bonds through urea-formaldehyde microcapsules having modified GO as core material in the epoxy system. There are several candidates for the modification of GO, but it was intended to use cost-efficient, eco-friendly, and biodegradable pigments obtained from green plants (leaves). Among all the plants, ***Catharanthus roseus* L.** of Apocynaceae family, commonly known as rose periwinkle, was taken to arrive at the mentioned goal. The leaves of this plant showed an inhibition efficiency of about 70% on steel surface [35]. The chosen leaves containing various organic moieties (9,12,15- Octadecatrienoic acid, Phytol, 1,2-Benzenedicarboxylic acid,diioctyl ester) were previously studied as a corrosion inhibitor. But, the effects of GO sheets modified by the chosen leaf extract on the adhesion behavior have not been still reported in the literature.

This work introduces a new strategy for improving corrosion inhibition by strengthening the adhesion bonds between the epoxy system and steel substrate. The structural change of GO sheets by various compounds in leaves extract was assumed to provide a strong bonding between the epoxy film and metal substrate through the ring-opening reaction of epoxy groups present in the polymer resin, which increases adhesion strength [9] between the coating and steel substrate. First, Graphene oxide modified by leaves extract was introduced into the epoxy matrix and fabricated on the steel surface. The modified GO sheets were studied by Fourier Transform Infrared Spectroscopy, Scanning Electron Microscopy, and Energy Dispersive X-ray analysis, and DFT modeling. The effect of GO-C.R/Epoxy film on the anti-corrosion properties of the neat epoxy coating was evaluated by electrochemical impedance spectroscopy. Second, GO-C.R sheets encapsulated in urea-formaldehyde microcapsules were synthesized by using the emulsion polymerization method. The prepared microcapsules were characterized by Fourier Transform Infrared Spectroscopy, the thermal stability of core material by Thermogravimetric analysis, and morphology of the microcapsules by Scanning Electron Microscopy. The effect of microcapsules in the epoxy matrix on the anticorrosion properties and adhesion strength of the coating was investigated by electrochemical impedance spectroscopy, salt spray test, and peel-off Test.

2. Experimental

2.1. Materials and Methods

Catharanthus roseus L. leaves were collected from Coimbatore District. All the chemicals and solvents were purchased from Sigma-Aldrich and used without advanced purification. The mild steel samples of dimensions 50 × 10 × 0.05 mm and the composition being 0.09 % C, 0.2 % Mn, 0.01 % S, 0.02% P, 0.01% N and 99.67% Fe were used. The epoxy value, solid content, and density of purchased epoxy resin were 0.1477-0.1665, 75-79% and, 0.96 g/cm^3, respectively. Epoxy resin and polyamide used for the coating purpose were purchased from Covai Seenu & Company. Before the coating process, the steel substrates were sand-blasted by SiC papers of grades 2000 and 2400 followed by degreasing the substrates with acetone. Then, the steel samples were thoroughly washed with water before proceeding with the coating process.

2.2. Synthesis of graphene oxide (GO)

Graphene oxide was synthesized by modified Hummer's method through oxidizing and exfoliating the graphite powder [26,36,37]. Accordingly, 1g of graphite powder was added to 60 mL of sulfuric acid under constant stirring at room temperature. After 2h, 6 g of potassium permanganate was added gradually to the solution within 1 h by maintaining the temperature below 20 °C. After that, the mixture was stirred at 35 °C for 6 h and as the reaction proceeded; the color turned from black to brown. Then, the mixture was diluted by the gradual addition of 200 mL of deionized water. After 2h, 10 mL of 30% hydrogen peroxide was added, to terminate the oxidation reaction. The mixture was centrifuged at 3500 rpm for 10 minutes and purified by washing several times with 1M hydrochloric acid and deionized water to remove acids and metal ions. The resulted oxidized product dispersed in deionized water was subjected to ultra-sonication for exfoliation. Finally, the graphene oxide powder was filtered and dried.

2.3. Preparation of Catharanthus roseus L. (C.R) extract

Catharanthus roseus L. leaves were washed thoroughly with distilled water and chopped into pieces. About 25 g of *Catharanthus roseus* L leaves were separately treated with 100 mL of Methanol and kept in an airtight container at 25 °C for 24 h. The extract was filtered by using filter paper and stored in an airtight jar for further studies.

2.4. Treatment of graphene oxide with plant extract

0.5 g of graphene oxide was dispersed in deionized water by sonication for 1 h at room temperature. About 20 mL of the prepared extract was added and stirred for 2 h. Then, the mixture was centrifuged and washed with distilled water three times to remove free extract molecules. The obtained residue was named GO-C.R.

2.5. Preparation of GO/C.R/Epoxy coatings and fabrication of steel substrates

To preparing decorated epoxy coatings, 30 mg of GO and GO-C.R sheets were separately dispersed through ultra-sonication in 10 mL distilled water and these dispersed solutions were added to 30 g of epoxy resin. To enable uniform dispersion of GO and GO-C.R composites in epoxy resin, they were treated with 6 mL of Dimethylformaldehyde and subjected to sonication for 30 min. In this way, GO and GO-C.R composites migrate from the aqueous phase to the epoxy phase (Wet Transfer Process) [38]. Then, the removal of water molecules trapped into the epoxy matrix was done by heating the mixture to 70 °C in an oven for 72 h. At last, polyamide hardener was mixed with a thick mass of GO and GO-C.R composites (w/w 1:2, respectively) and fabricated onto the surface of sandblasted steel substrates. The coating was dried at room temperature for 24 h followed by curing at 120 °C in an oven for 6 h. The dry thickness of the coating was found to be 0.055 mm.

2.6. Synthesis and application of UF-GO/GO-C.R microcapsules on the steel samples

Urea-formaldehyde microcapsules comprising GO/GO-C.R were prepared by in situ polymerization reaction of formaldehyde with urea. Urea (2.4024 g), Resorcinol (0.12 g), and Ammonium chloride (0.12 g) were dissolved in 50 mL of deionized water where Resorcinol act as a cross-linking agent and Ammonium chloride was added to improve the strength and shell formation of microcapsules [42]. 0.05 g of GO/GO-C.R sheets was dispersed using an ultrasonicator for 5 minutes in 10 mL of deionized water. Then, GO/GO-C.R suspensions were individually added to the microcapsule solution. After that, pH of the solution was attuned to 3.5 with HCl solution, and 10 mL epoxy resin was added drop-wise into mixing microcapsule solution. This solution was stabilized by mixing at 800 rpm for 15 mins with a stirrer. Then, 2.0 mL of formaldehyde solution was added to the stabilized solution. The temperature was increased to 60°C, and the reaction was carried out for 4 hours. The reaction solution was cooled to room temperature and filtered. The microcapsules obtained were purified with deionized water and acetone and dried at room temperature. The dried microcapsules dispersed in N,N-Dimethylformamide using ultrasonication were transferred to the epoxy matrix via wet transfer method. The mixture was placed at 80 °C for 48 h in an oven for removing N, N-Dimethylformamide. Later, UF-GO/Epoxy and UF-GO-C.R/Epoxy sheets were treated with a hardener in the ratio of 2:1 (w/w) and applied on the pre-cleaned (blasted by sandpapers followed by acetone degreasing) steel surface. The coated substrates were dried at room temperature for 24 h followed by curing in the oven for about 6 h at 100 °C. The dry thickness of the coated specimens was 0.055 mm.

3. Characterizations

FT-IR analyses were employed for the characterization of GO and GO-C.R composites. FT-IR measurements were carried out (KBr disk, 4000-400 cm^{-1}) by SHIMADZU spectrometer. It was recorded also to evaluate the extent of bonding between pure epoxy and modified GO/epoxy coatings. To evaluate the chemical reactivity of phyto-components on the surface of GO sheets towards the corrosion inhibition process, DFT studies were executed. The green compounds were optimized and relaxed using Density Functional studies (DFT) based on **B3LYP** procedure with **6-31G (d, p)** basis functional sets [39] using **Gaussian 09** software program. The surface wettability of the modified GO/epoxy coating substrates at the humidity of 30% and room temperature were determined using OCA 20 video-based contact angle measurement unit. In this measurement, a Canon-type digital camera was used to record the shape and contact angle of the water droplet placed on the coating surface after 10s. The effect of GO and GO-C.R embedded microcapsules on the corrosion defensive properties was explored by utilizing electrochemical impedance spectroscopy (EIS) and polarization technique at room temperature. The analyzes were made in 3.5% NaCl solution at different immersion phases as per standard ASTM G-72[43]. The EIS measurements were carried out with the help of three-electrode set-up containing platinum electrode as a counter electrode, saturated calomel electrode as a reference electrode, and coated substrates as a working electrode having an area of ~ 1cm [2] at OCP (100 kHz-10 mHz) and a sinusoidal amplitude of 10 mV. All the measurements were exerted using NOVA Auto lab (version 6) software.

Thermal stability of the synthesized microcapsules was evaluated using thermo-gravimetric and differential thermal gravimetric analyzes by thermo-gravimetric analyzer (PerkinElmer, TGA 400). For this experiment, 4-6 mg of the sample was taken and mass loss was observed over the temperature range of 25-700 °C with a heating rate of 5 °C/min, in nitrogen atmosphere.

The surface interactions and wettability nature of pure epoxy and epoxy composites containing GO and GO-C.R microcapsules were inspected by contact angle measurements. For this motive, OCA 20 video-based contact angle determining unit was used. The effect of epoxy coatings on the mild steel substrate was investigated by carrying out Salt spray test by following ASTM B117 international standard. A X-shaped scribe with a width of 1mm and length 2.5 cm was fashioned by using a penknife on the epoxy coating and placed at 45° in the test chamber. And, samples were constantly sprayed with 5.0% NaCl solution for 300 h at pH and temperature of 6.5–7.2 and 35±2 °C, respectively. The condensate collected in the cabinet was at the rate of 1.0–2.0 mL/h.

Peel off test was performed to measure the adhesion strength of coating on the mild steel substrates by following ASTM D 4551 procedure. In this test, a Polyimide Kapton Tape was made to adhere to the surface of the substrates and the strip was peeled off at 90° with a constant force. The force of detachment was measured with respect to displacement and the coating was detached at the rate of 10mm/min.

4. Results

4.1. Characterization of GO and GO-C.R sheets

4.1.1. FT-IR Analysis

The structural changes observed through the functionalization of GO sheets with C.R leaf extract were evidenced by recording the FT-IR spectrum. FT-IR spectra of GO and GO-C.R sheets were displayed in Fig. 1. In the spectrum of GO, broadband at 3658 cm^{-1} was observed,

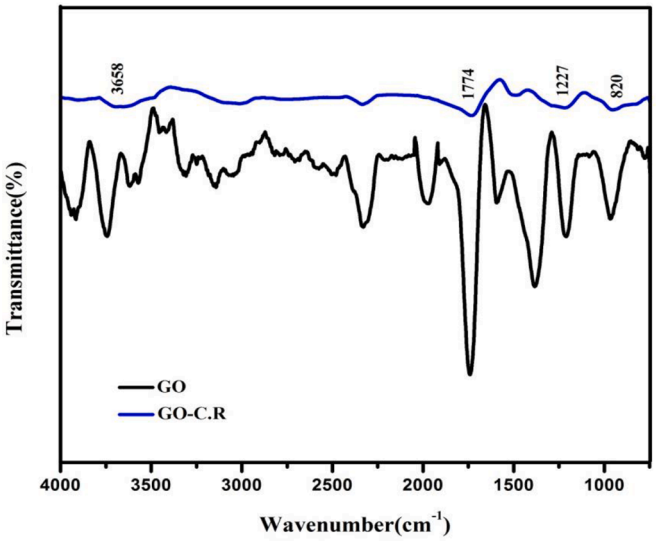

Fig. 1. FT-IR Spectra of GO and GO-C.R.

which was attributed to the presence of hydroxyl moiety. The peaks at 1346, 1774, and 3047 cm^{-1} were assigned to the stretching of C-O, C=O, and –OH bonds of the carboxylic acid group, respectively. Two separate sharp peaks at 820 and 1227 cm^{-1} correspond to the stretching of C-O-C bonds, which are related to the presence of the epoxy group. These peaks indicated the proper functionalization of GO with various moieties that counterparts well with literature. An absorption frequency at 1764 cm^{-1} was assigned to C=O stretching, peaks at 1265, 2889, and 1417 cm^{-1} were attributed to the existence of C-O-C, CH_3 symmetric, and CH_3 (gem dimethyl) stretching, respectively. FT-IR spectrum of GO-C.R shows the absorption frequencies related to both GO and crude C.R leaf extract [49]. This evidenced the successful modification of GO by crude C.R leaf extract. Further, the visual pictures of the aqueous suspension stability after 48 h are provided in Fig. 2. GO suspension remains stable for over 48 hr, which denotes the occurrence of hydrophilic groups like carbonyl and hydroxyl groups on the surface of GO whereas, the unstable nature of GO-C.R attributes to the existence of hydrophobic groups.

4.1.2. Field Emission Scanning Electron Microscopy (FE-SEM) analysis

The effect of modification on the surface morphology of GO was analyzed by FE-SEM analysis. Micrographs provided in Fig. 3a & b showed irregular folding on GO. This evidenced that, during the oxidation process, graphite has undergone an exfoliation process. This may be because of the result of structural changes of graphite to figure out graphene oxide [36]. After the process of modification, the crumbled structures of GO sheets have been buckled into layered structures via the restacking process. It is apparent from these results that the modification process has a large effect on the surface morphology of GO sheets.

4.1.3. Energy Dispersive X-ray (EDX) studies

The EDX spectrum of GO sheets shows various peaks corresponding to carbon (69.8%), oxygen (29.93%), silicon (0.05%) and Sulfur (0.21%). Upon the modification, GO-C.R (Fig. 3a & b) showed an increase in the atomic percentage of carbon and a decline in the percentage of oxygen in comparison with GO sheets. The atom ratio of C:O of GO and GO-C.R were calculated to be 1.39: 0.59 and 1.48: 0.50, respectively. This confirmed the successful modification of GO sheets by phytocomponents of C.R extract.

4.1.4. DFT Studies

The interactions between green molecules of *Catharanthus roseus* L. leaves extract with GO were investigated by employing DFT modeling. The optimized clusters of Phytol, 1,2-Benzenedicarboxylic acid,diioctyl ester, 9,12,15- Octadecatrienoic acid ([Table 1) over GO surface were displayed in [Fig. 4. All the selected phytocompounds get stabilized near GO, proving their attraction towards the upper surface of GO. It is clear from the resulting clusters that GO adsorbed phytocompounds through H-bonds via –OH groups on GO surface. Also, 1,2-Benzenedicarboxylic acid, diioctyl ester with an aromatic backbone lies parallel to GO surface due to π- π interactions. The adsorption tendency of green compounds were evaluated via calculating the binding energy term. The binding energy of Phytol(-21.67 kcal/mol), 1,2-Benzenedicarboxylic acid, diioctyl ester (-33.29 kcal/mol), 9,12,15- Octadecatrienoic acid (-27.41 kcal/mol) on adsorption over GO was calculated. The negative binding energy values disclose the successful adsorption of phytocompounds on GO surface. Among all the three selected phytocompounds, 1,2-Benzenedicarboxylic acid,diioctyl ester was known to possess higher negative energy proving that it has higher affinity towards GO owing to their chemical adsorption (π- π interactions) on the surface.

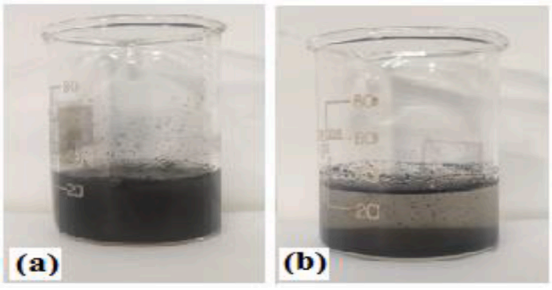

Fig. 2. Visual images of the stability of (a) GO and (b) GO-C.R sheets after 48h.

4.2. Characterization of GO-UF/GO-UF-C.R microcapsules

4.2.1. FT-IR analysis

FT-IR spectra of UF-GO and UF-GO-C.R microcapsules were displayed in [Fig. 5. Absorption bands at 3337 cm^{-1}, 1600 cm^{-1}, and 1515 cm^{-1} correspond to N-H stretching, N-H bending, and C=O bending frequencies of urea in poly(urea-formaldehyde) shell of UF-GO and UF-GO-C.R microcapsules. Epoxy resin as a core material was noticed at 1029 cm^{-1} and 2963 cm^{-1} attributed to sp [3] C-H stretching. These bands show the thriving encapsulation of GO and GO-C.R to microcapsules. Owing to the peak overlapping [42] and its lower percentage in composition peaks corresponding to GO could not be observed.

4.2.2. FE-SEM analysis

Fig. 6 shows the surface morphology of microcapsules, which was analyzed by using SEM analysis. Typically, the microcapsules were observed to be spherical, which guaranteed the storage space inside the capsules [43] and also assured pronounced dispersion of microcapsules in the neat epoxy matrix. The outer surface of the microcapsules was rough in consequence of the extending nature of the urea-formaldehyde capsule core. Also, core material enhanced the surface area and adhesion strength of the capsules. The size of the microcapsules may vary with the amount of urea-formaldehyde deposition on the core material.

4.2.3. TGA-DSC analysis

The thermal behavior of UF-GO and UF-GO-C.R microcapsules was investigated by Thermogravimetric analysis (TGA) are shown in Fig. 7. The first degradation was observed from 280 up to 320 °C and 213 up to 319 °C attributing to DSC inflection point at 272 °C and 291 °C, respectively for UF-GO and UF-GO-C.R microcapsules which shows that both are stable up to 270 °C. This degradation can be ascribed to persuade thermal decomposition of shell material and after this temperature, cross-linking and depolymerization reactions may have occurred. Further, degradation of monomers and the evolution of methane, carbon dioxide, and ammonia as gaseous products can be expected. Also, there observed two-step degradation that proved the existence of GO and GO-C.R in poly (urea-formaldehyde) core. This degradation was noticed from 320 up to 470 °C and 353 up to 438 °C corresponding to DSC inflection point at 360 °C and 413 °C, respectively for UF-GO and UF-GO-C.R indicating the degradation of formaldehyde from the capsule shell. The weight loss was observed beyond 460 °C which results from the presence of core (anti-corrosion) material in the microcapsules providing the evidence for the encapsulation of GO and GO-C.R sheets by urea-formaldehyde shell. Prepared microcapsules reveal a higher weight loss percentage at second stage degradation because of the higher content of GO and its derivative.

4.3. Evaluation of corrosion behavior of GO/GO-C.R epoxy coated substrates

4.3.1. Potentiodynamic polarization measurements

The anti-corrosion efficiency of various epoxy-based coatings was estimated by performing Tafel analysis for the samples immersed in 3.5 % sodium chloride solution after 7 days at 298 K. Fig. 8 shows the cathodic and anodic potentiodynamic curves of untreated/Epoxy, GO/Epoxy and GO-C.R/Epoxy treated steel substrates. The corrosion parameters such as E_{corr} (corrosion potential), i_{corr} (corrosion current

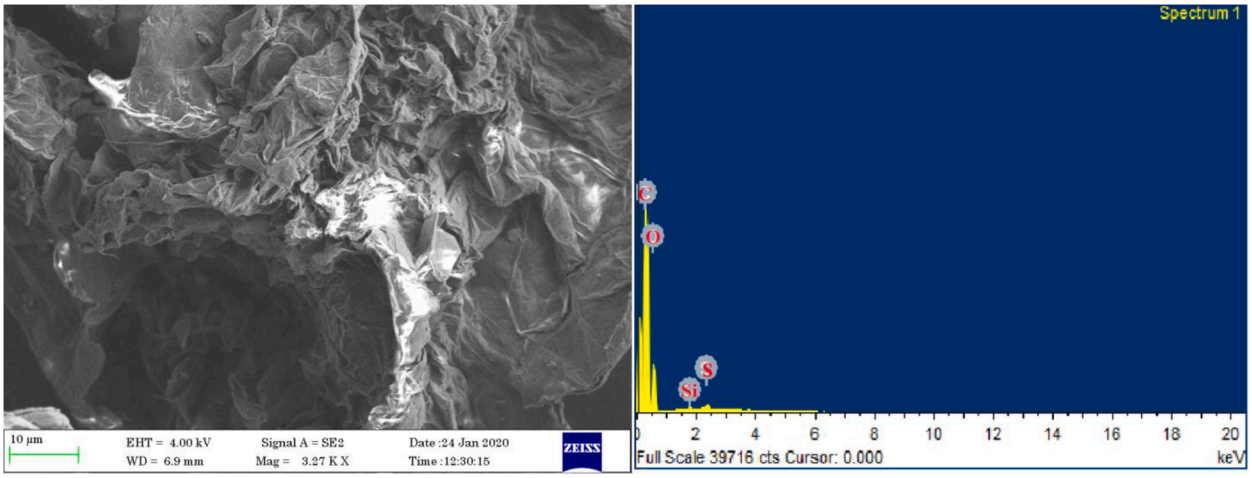

SEM and EDX images of GO

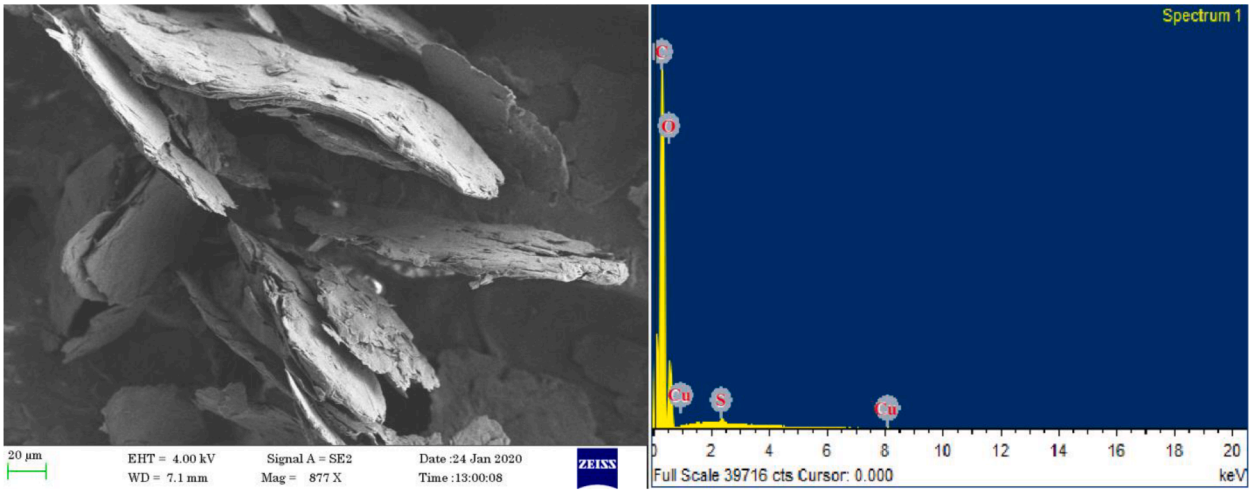

SEM and EDX images of GO-C.R

Fig. 3a. (a)SEM and EDX images of GO.
(b)SEM and EDX images of GO-C.R.

Table 1
Phytocompounds used to modify the structure of GO in the present investigation.

S. No.	Name of the Phytocompounds	Structures
1.	Phytol	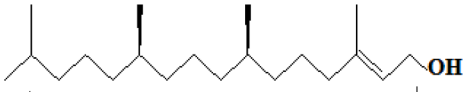
2.	1,2-Benzenedicarboxylic acid,diioctyl ester	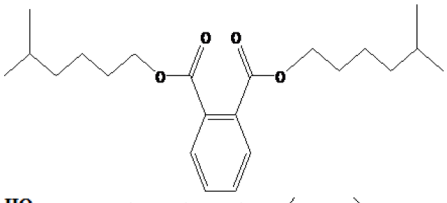
3.	9,12,15-Octadecatrienoic acid	

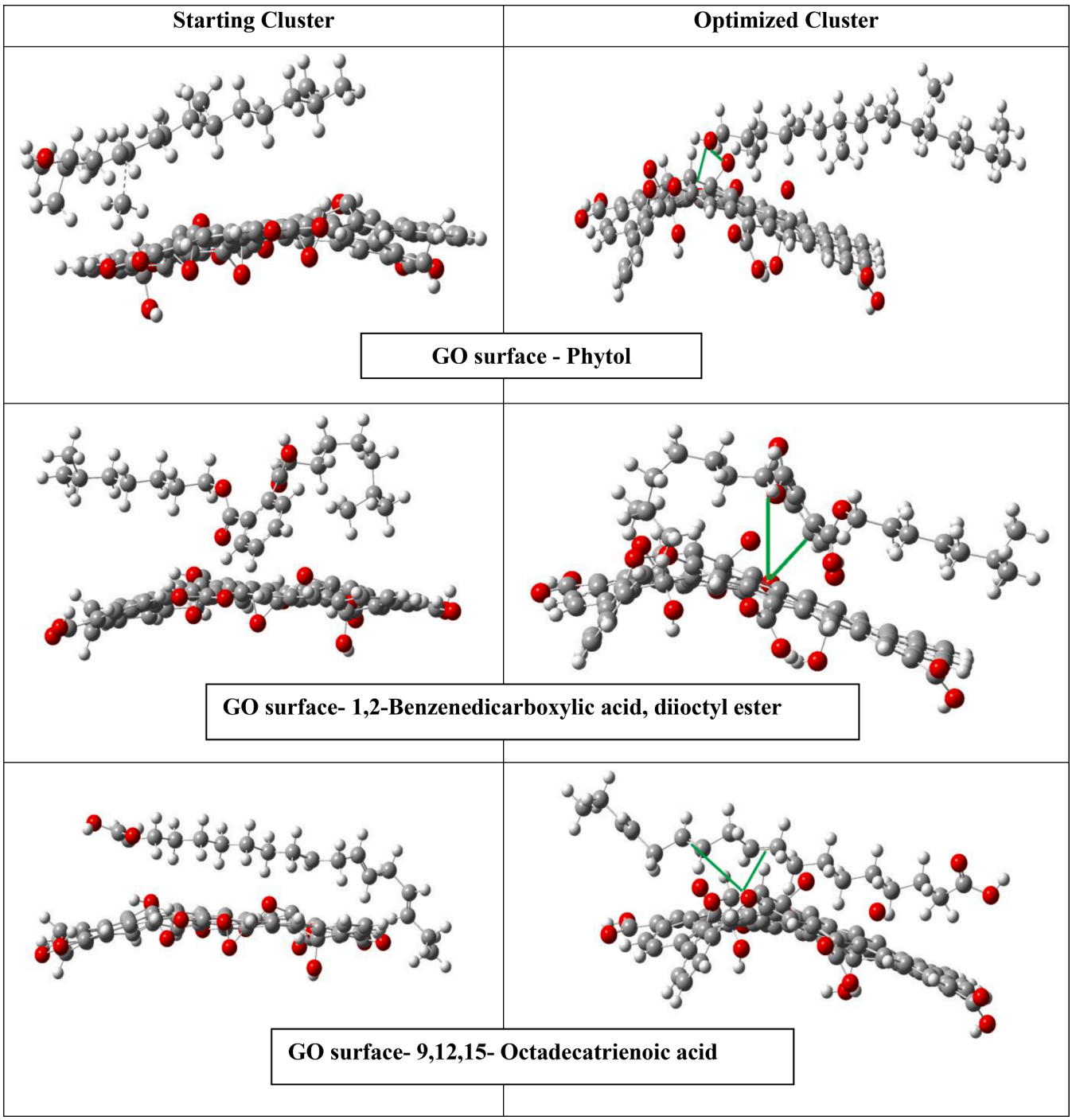

Fig. 4. The optimized geometries of Phytol, 1,2-Benzenedicarboxylic acid,diioctyl ester, 9,12,15- Octadecatrienoic acid over GO surface. The interactions are shown in blue lines.

density), βa, and βc (anodic and cathodic Tafel slopes) are determined from extrapolation of Tafel curves and R_p (polarization resistance) for all the samples were recorded in Table 2. From the results, it is apparent that E_{corr} values of GO-C.R/Epoxy (-0.5395 V) shift towards a more positive potential value after the immersion time of 7 days, when compared to the untreated/Epoxy sample (-0.7115 V). The i_{corr} value (1.01 μA/cm^2) for GO-C.R/Epoxy is more meager than untreated/Epoxy steel (238 μA/cm^2) and which is reduced two-fold compared to GO/Epoxy (3.09 μA/cm^2) after 48 h exposure to 3.5% NaCl solution. Also, the polarization resistance value of GO-C.R/Epoxy is much higher than both the other substrates. Besides, the cathodic Tafel slope of untreated/Epoxy steel is more enhanced compared to that of modified epoxy coatings, suggesting that the addition of GO and GO-C.R has inhibited the cathodic reaction [40]. The protection efficiency of modified epoxy-based coatings was estimated by using the following Eq. (1) [41]:

$$P_{EF}\% = \frac{i_{corr}(uncoated) - i_{corr}(coated)}{i_{corr}(uncoated)} \text{ x } 100\% \quad (1)$$

The efficiency of GO-C.R/Epoxy coating is found to be the highest (**62.2 %**).

4.3.2. OCP measurements

OCP measurements were conducted to examine and compare the

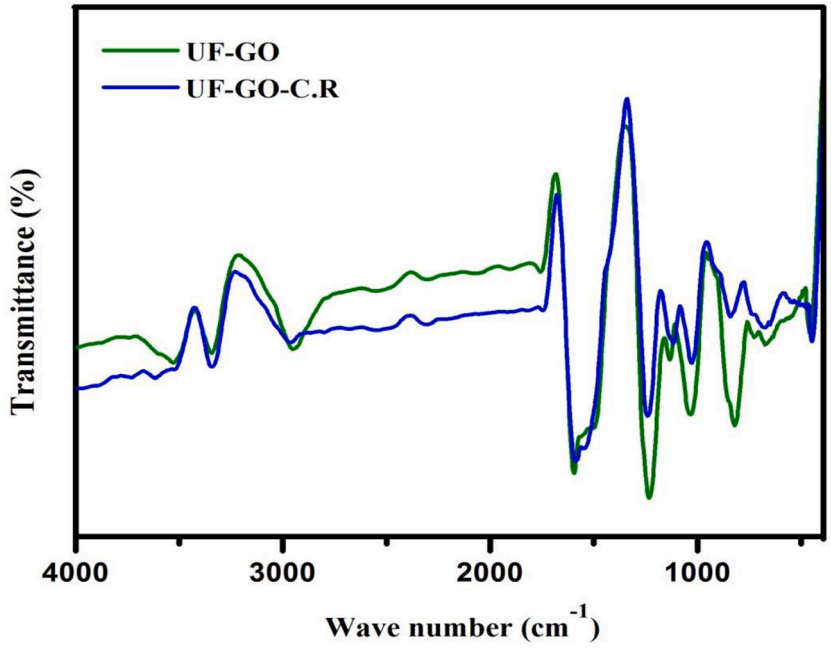

Fig. 5. FT-IR spectra of UF-GO and UF-GO-C.R microcapsules.

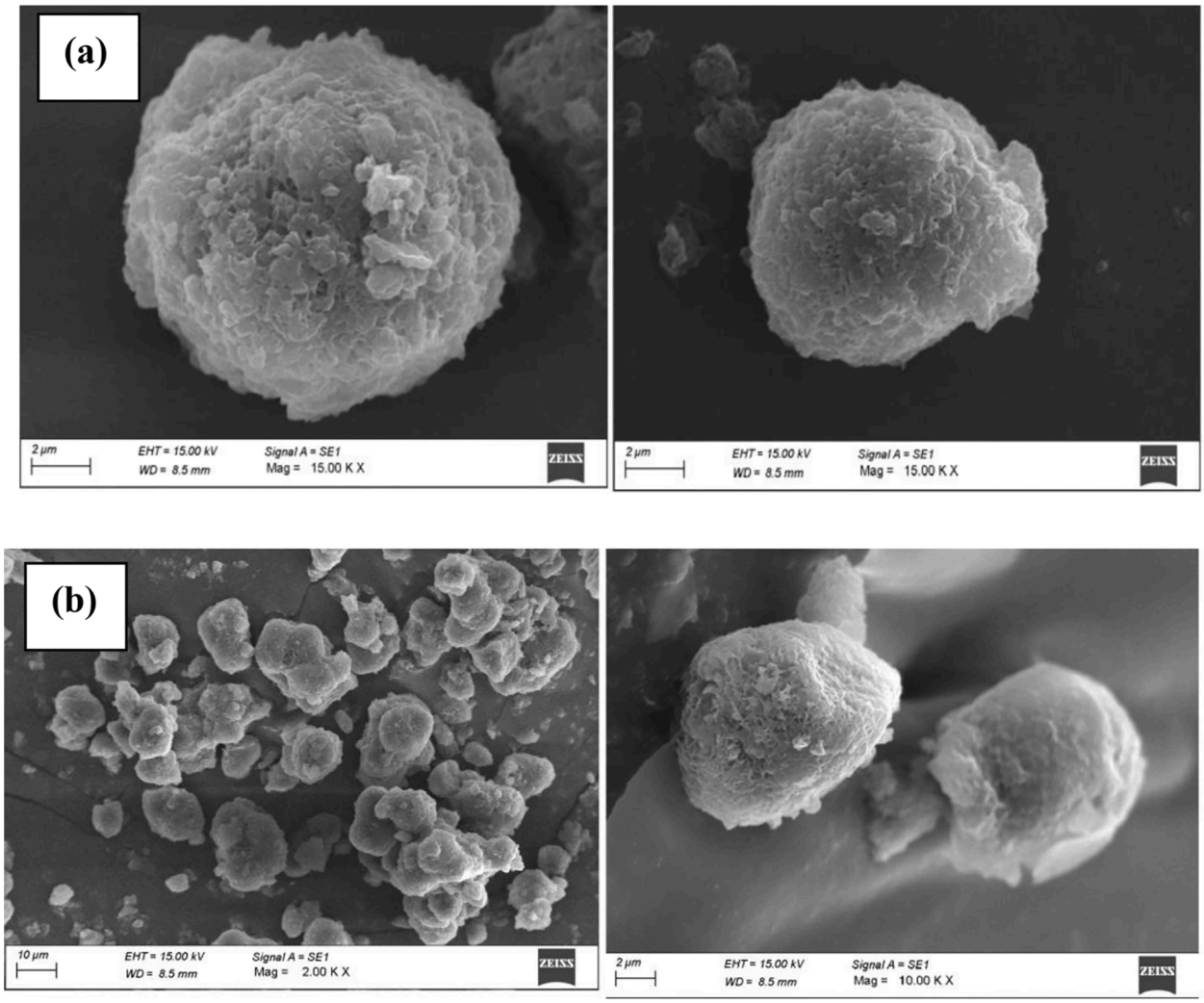

Fig. 6. SEM images of **(a)** UF-GO **(b)** UF-GO-C.R microcapsules.

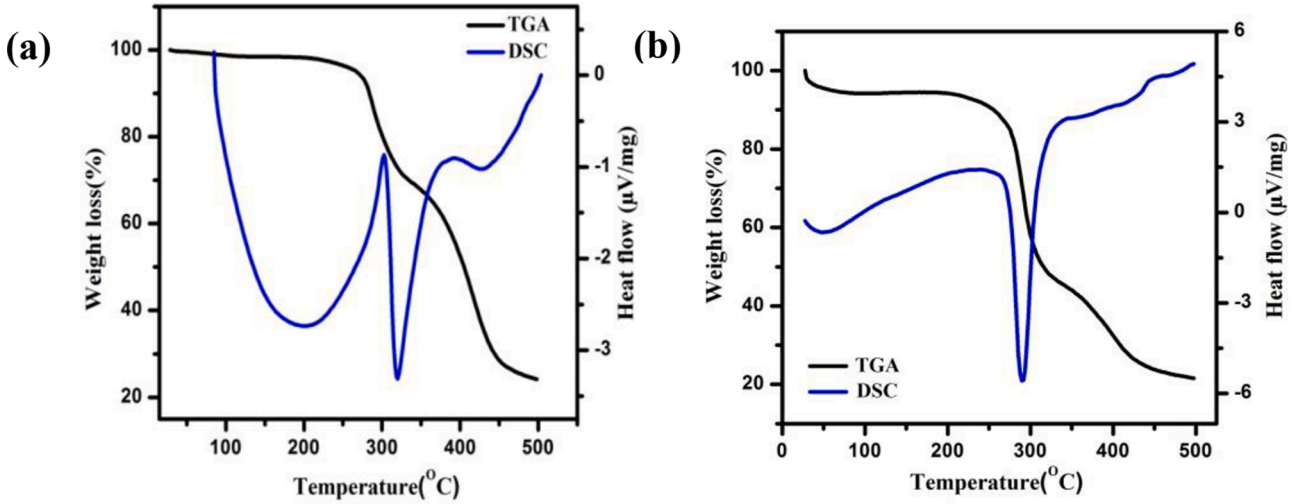

Fig. 7. TGA and DSC curves of **(a)** UF-GO **(b)** UF-GO-C.R microcapsules.

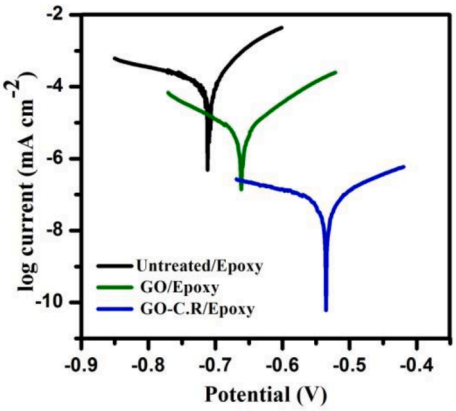

Fig. 8. Potentiodynamic polarization curves for Untreated/Epoxy, GO/Epoxy, and GO-C.R/Epoxy coatings exposed to 3.5 % NaCl after 7 days.

effects of the addition of GO and modified GO to neat epoxy coatings on the corrosion resistance performance of mild steel substrates immersed in 3.5% NaCl solution at various periods of 1 h, 1 d, 3 d, 5 d & 7 d. Fig. 9 shows the OCP values for untreated epoxy, GO/Epoxy, and GO-C.R/Epoxy coatings at different intervals. It is clear from Table 2 that OCP values shift to negative values because of an increase in immersion time for all the samples. This may be because of the ingress of electrolyte through the film. However, the metal substrate coated with GO-C.R/Epoxy coatings shows more positive OCP values at all immersion times when compared to other samples. This suggests that the addition of GO-C.R to the epoxy matrix may increase the barrier performance of the coating by decreasing the intrusion of corrosion electrolyte through the metal/coating interface [20].

4.3.3. Corrosion performance of coating system by electrochemical studies

The Nyquist plots of untreated/Epoxy, GO/Epoxy and GO-C.R/Epoxy coatings after different immersion periods in 3.5% NaCl solution are displayed in Fig. 10. The electrical circuit used for fitting the EIS data is shown in Fig. 18. The values of impedance parameters such as R_s (solution resistance), R_{ct} (charge transfer resistance), R_c (coating resistance), CPE_{dl}, and CPE_c (constant phase element of double layer and coating respectively) modeled in two time constant circuits are provided in Table 3. It is evident from the results that, as the immersion time increases, the values of log $|Z|_{100mHz}$ and R_c decreased for all substrates, showing the ingression of corrosion electrolyte into the surface of the substrates. However, GO-C.R/Epoxy coated sample showed a significant rise in the initial values of log $|Z|_{100mHz}$ and R_c when compared to the untreated/Epoxy sample. The total resistance values decreased for all the samples with the increase in immersion time, which is displayed in Fig. 15. The Nyquist plots (Fig. 6) reveal that the epoxy resin modified

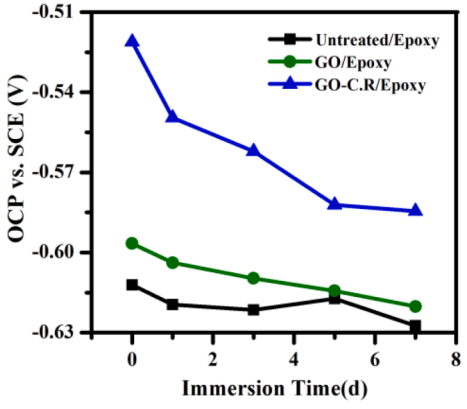

Fig. 9. OCP plots for Untreated/Epoxy, GO/Epoxy, and GO-C.R/Epoxy coatings exposed to 3.5 % NaCl after 7 days.

Table 2
Potentiodynamic parameters of the samples exposed to 3.5% NaCl after 7 days.

Samples	E_{corr} (V)	i_{corr} (μA/cm^2)	βa (V/dec)	βc (V/dec)	R_p(kΩ cm^2)	Thickness (mm)	P_{EF} (%)
Bare	-0.8993	18.9	0.3101	0.0765	0.090	0.055	-
Untreated/Epoxy	- 0.7115	9.8	0.2925	0.0801	0.601	0.055	48.1
GO/Epoxy	-0.6874	4.8	0.1988	0.0817	1.112	0.055	51.0
GO-C.R/Epoxy	-0.5395	3.7	0.1228	0.0945	2.845	0.055	62.2
UF-GO/Epoxy	-0.5929	3.6	0.1355	0.2016	1.947	0.055	63.3
UF-GO-C.R/Epoxy	-0.5483	1.6	0.3415	0.1488	10.672	0.055	83.6

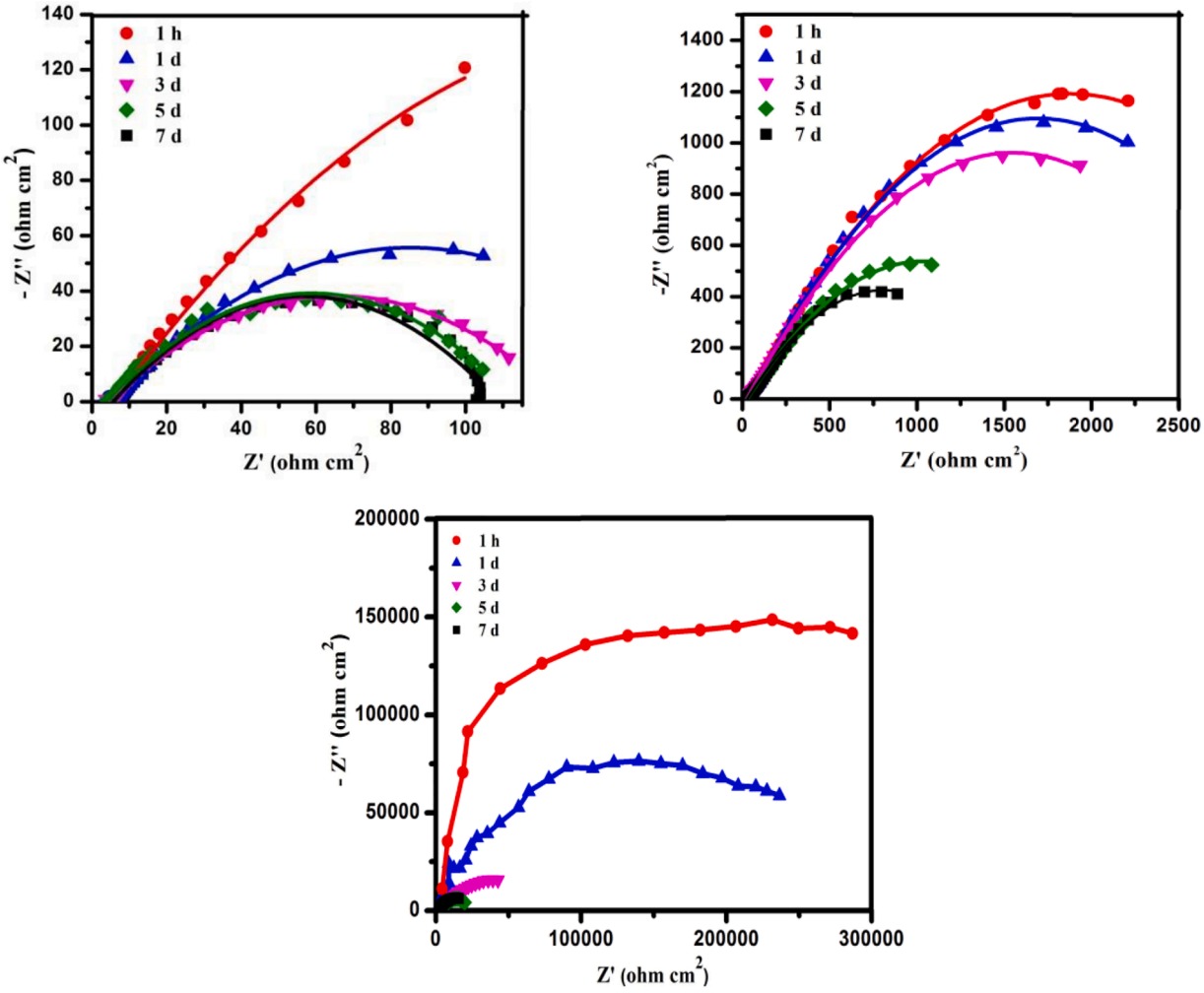

Fig. 10. Nyquist plot of Untreated/Epoxy, GO/Epoxy, and GO-C.R/Epoxy coated samples immersed in 3.5 % NaCl solution; Marker points and solid lines represent the experimental and fitted results, respectively.

by GO and GO-C.R sheets increased the modulus of phase angle (100 mHz) values at all immersion times. This leads to the activation of anti-corrosion performance for those samples, which may be due to the insulation of active cathodic sites on the metal surface. Therefore, this eliminates the destruction of adhesion bonds by preventing the penetration of corrosion agents to active sites. Also, GO-C.R/Epoxy coated sample showed the lowest decrease in the corrosion resistance activity (Table 3). This sample not only eliminates the diffusion of corrosion electrolyte but also promotes the anti-corrosion activity by strengthening the adhesion bonds between the epoxy coating and metal substrate.

4.4. Evaluation of corrosion behavior of UF-GO/UF-GO-C.R epoxy coated substrates

4.4.1. Potentiodynamic polarization measurements

The anti-corrosion efficiency of microcapsule contained epoxy-based coatings was estimated by performing Tafel analysis for the samples immersed in 3.5 % sodium chloride solution after 7 days at 298 K. Fig. 11a shows the cathodic and anodic potentiodynamic curves of untreated/Epoxy, UF-GO/Epoxy, and UF-GO-C.R/Epoxy treated steel substrates. From Table 2, it is clear that E_{corr} values of UF-GO-C.R/Epoxy (-0.5329 V) shift towards a positive potential value after the immersion time of 7 days, when compared to the untreated/Epoxy sample (-0.7115 V). The i_{corr} value for UF-GO-C.R/Epoxy (2.0 μA/cm^2) is reduced three-fold compared to UF-GO/Epoxy (3.6 μA/cm^2) after 7 days exposure to 3.5 % NaCl solution. In addition, the polarization resistance value of UF-GO-C.R/Epoxy coated sample is much higher than other substrates. The efficiency of GO-C.R/Epoxy coating was found to be the highest (**79.5 %**). Also, the steel substrate coated with UF-GO-C.R microcapsules showed positive values of OCP than all other samples at all investigation periods (Fig. 11b).

4.4.2. Electrochemical studies

The Nyquist plots of untreated/Epoxy, UF-GO/Epoxy, and UF-GO-C.R/Epoxy coatings after different immersion periods in 3.5% NaCl solution are displayed in Fig. 12. The values of impedance parameters such as R_s (solution resistance), R_{ct} (charge transfer resistance), R_c (coating resistance), CPE_{dl}, and CPE_c (constant phase element of double layer and coating respectively) modeled in two time constant circuits are provided in Table 3. It is apparent from Table 3 that UF-GO-C.R/Epoxy sample showed a decrease in the values of log $|Z|_{100mHz}$ and R_c until 5d evidencing the intrusion of corrosion solution into the surface of the substrates and after that, the sample showed an increase in values indicating the formation of protective barrier. The total resistance values increased for epoxy coatings with GO-C.R microcapsules than other samples, which are displayed in Fig. 15. The Nyquist plots (Fig. 12) reveal that the epoxy resin modified by GO and GO-C.R introduced microcapsules increased the modulus of phase angle (100 mHz) values at all immersion times than neat epoxy coated sample. This may be due to the creation of anti-corrosion performance on those samples by casing the cathodic sites at the steel surface. As a result, the annihilation of

Table 3
Electrochemical parameters obtained from EIS analysis.

Sample	ImmersionTime	R_{ct} (ohmcm [2])	R_c (ohm cm^2)	Rt(ohm cm^2)	log$\|Z\|_{100mHz}$(ohm cm^2)	-θ $_{100kHz}$(deg)	OCP vs. SCE (V)
Untreated/Epoxy	1h	1780	86.4	1866.4	3.39	21.03	-0.6122
Untreated/Epoxy	1d	1780	107	1887	3.38	17.87	-0.6195
Untreated/Epoxy	3d	1520	93.2	1613.2	3.33	18.99	-0.6215
Untreated/Epoxy	5d	815	81.6	896.6	3.08	16.61	-0.6173
Untreated/Epoxy	7d	677	65.3	742.3	2.99	15.3	-0.6274
GO/Epoxy	1h	2820	126	2946	3.58	21.99	-0.5966
GO/Epoxy	1d	2590	146	2736	3.53	18.73	-0.6038
GO/Epoxy	3d	2360	131	2491	3.51	21.19	-0.6097
GO/Epoxy	5d	1670	107	1777	3.35	18.53	-0.6143
GO/Epoxy	7d	1050	47.4	1097.4	3.18	18.43	-0.6202
GO-C.R /Epoxy	1h	3589	146	3735	3.26	40.64	-0.5623
GO-C.R /Epoxy	1d	3167	114	3281	3.20	33.17	-0.5734
GO-C.R /Epoxy	3d	3098	107	3207	3.02	24.54	-0.5778
GO-C.R /Epoxy	5d	3593	345	2938	3.41	69.20	-0.5748
GO-C.R /Epoxy	7d	2960	321	2281	4.06	37.52	-0.5860
UF-GO/Epoxy	1h	4090	4510	8600	3.58	32.46	-0.5820
UF-GO/Epoxy	1d	3410	3940	7340	3.49	44.39	-0.5914
UF-GO/Epoxy	3d	2210	2590	4800	3.38	50.22	-0.5988
UF-GO/Epoxy	5d	2120	1971	4091	3.36	45.74	-0.5996
UF-GO/Epoxy	7d	1876	1190	3066	3.28	43.41	-0.6028
UF-GO-C.R/Epoxy	1h	12700	5250	17950	6.56	76.48	-0.5210
UF-GO-C.R/Epoxy	1d	12876	4981	17857	5.38	69.88	-0.5495
UF-GO-C.R/Epoxy	3d	11863	4523	16386	4.23	58.47	-0.5620
UF-GO-C.R/Epoxy	5d	10983	3982	14965	4.30	60.61	-0.5821
UF-GO-C.R/Epoxy	7d	10688	4981	15669	4.66	66.46	-0.5845

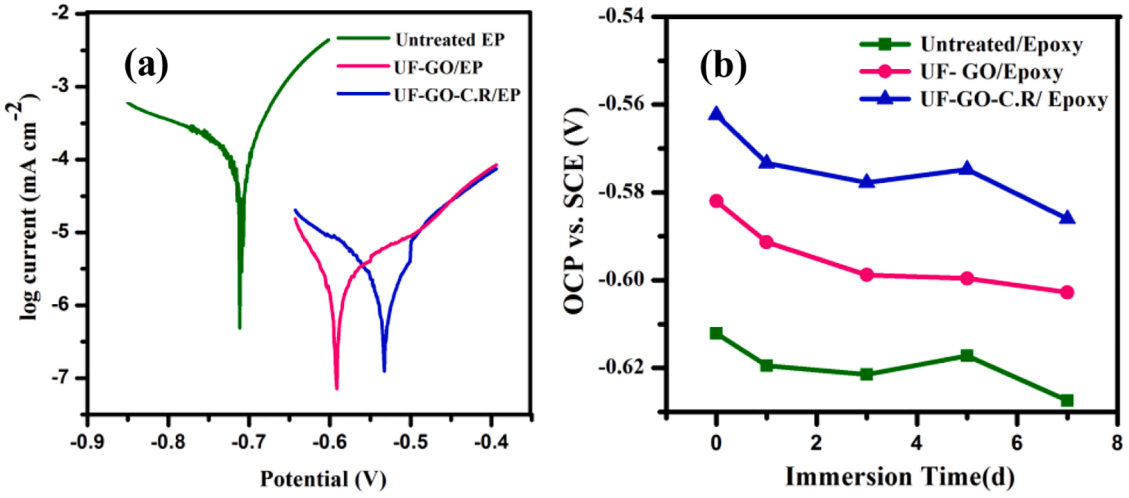

Fig. 11. **(a)** Potentiodynamic polarization curves and **(b)** OCP plots for Untreated/Epoxy, UF-GO/Epoxy, and UF-GO-C.R/Epoxy coatings exposed to 3.5 % NaCl after 7 days.

adhesion bonds by the penetration of corrosion agents to active sites could be avoided to the maximum extent.

4.5. Salt Spray Test

Fig. 13 displays the visual pictures of the effect of upper epoxy coatings treated with UF-GO and UF-GO-C.R on the anti-corrosion performance after 144 and 300 h of continuous exposure to 5.0 % NaCl solution in salt spray cabinet. From the results, the accumulation of corrosion agents and blisters was found around the scribe on the substrate without GO treatment. The increase of spray period to 300 h resulted in the complete erosion of epoxy coatings. This may be because of the diffusion of corrosive agents to the substrate coating interface through the microstructures present on the coatings. But, in the UF-GO microcapsules added epoxy coatings, fewer corrosion products are observed around the scratch and on the increase in exposure time, more blisters were observed around the scratch. However, at all exposure times, UF-GO/Epoxy coating has fewer blisters than the untreated/Epoxy coating.

4.6. Contact angle measurements

The wettability and relative interactions of epoxy coatings and the coatings modified by UF-GO and UF-GO-C.R were quantified by measuring the contact angle between the samples and a sessile water droplet. The outcome of this measurement, including the surface free energy (W_a) and the water contact angle(θ) for all the samples, were predicted by using Neumann equation [44] are provided in Table 4 and Fig. 14. Results reveal noticeably that the lowest value of contact angle and the highest values of surface free energy correspond to the unmodified epoxy coated steel substrate. Also, the modification of epoxy coatings with UF-GO and UF-GO-C.R has resulted in the increase of

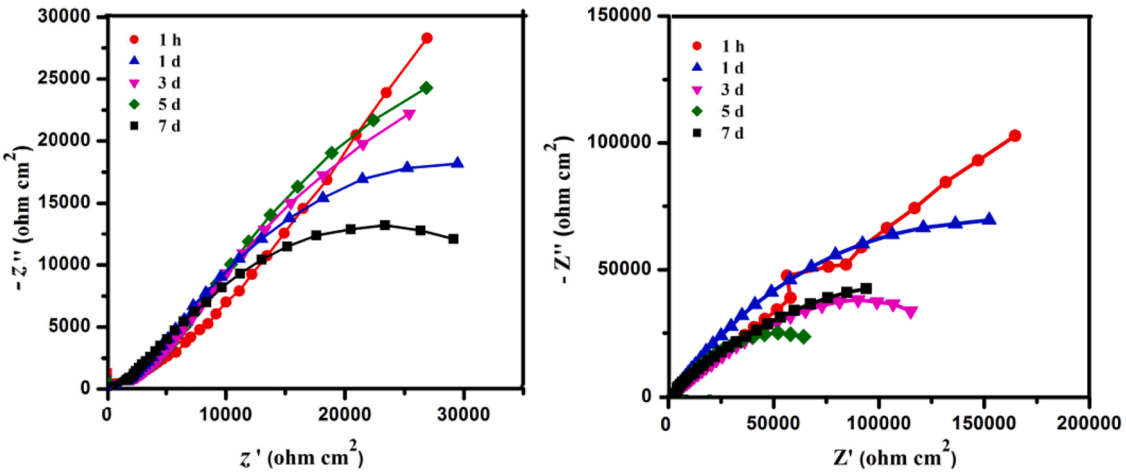

Fig. 12. Nyquist plot of UF-GO/Epoxy, and UF-GO-C.R/Epoxy coated samples immersed is 3.5 % NaCl solution; Marker points and solid lines represent the experimental and fitted results, respectively.

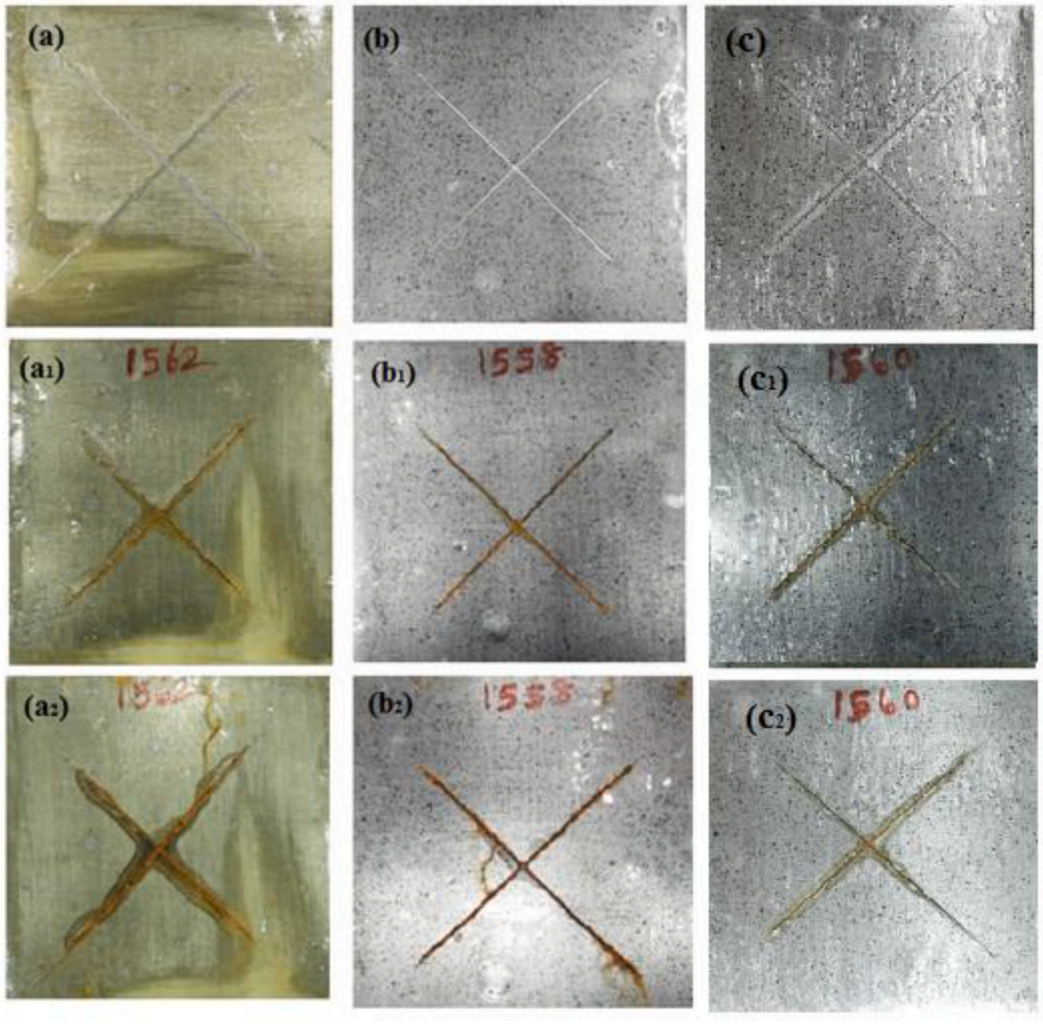

Fig. 13. Visual performance of salt spray test of scratched steel substrates (a) Untreated/Epoxy (b) UF-GO/Epoxy (c) UF-GO-C.R/Epoxy after 144 and 300 h exposure to 5.0 % NaCl solution.

contact angle from 68.2 to 78.7 and 84.8, respectively, and the decrease in W_a values.

4.7. Adhesion measurements

To carry out the peel off mechanical test, the coated samples with the tape were struck was assembled. At the initial stage of this process, the

Table 4
Results drawn from contact angle measurements on Untreated/Epoxy, UF-GO/ Epoxy, and UF-GO-C.R/Epoxy coatings.

Sample	θ (°)	W_a (mJ/m^2)
Untreated/Epoxy	68.2	98.7
UF-GO/ Epoxy	78.7	86.1
UF-GO-C.R /Epoxy	84.8	78.5

load (*N*) applied to peel off the tape, and that was found to increase with an increase in the displacement (constant plateau region). This stage was followed by the steady-state stage where the fluctuations in load are observed. These fluctuations reflected the stability and adhesion strength with which the coating adheres itself to the steel surface. From Table 5, the maximum adhesion strength (290 N) was observed for UF-GO-C.R/Epoxy sample.

5. Discussion

The surface of GO sheets is hydrophilic, which is attributed to the existence of various functionalities, such as hydroxyls, carboxyls, and epoxides. The strong π- π interactions and larger surface area of GO sheets result in poor dispersion with the epoxy matrix, which results in the ingression of corrosive ions into the metal/coating interface. However, GO sheets grafted by inhibitor components exhibit hydrophobic nature, making them excellent for dispersion in the polymer matrix. Besides the behavior of GO-C.R sheets as corrosion inhibitors, they can also influence the performance of the potential barrier to epoxy resin. The strengthening of adhesion bonds between the metal substrate and GO-C.R sheets takes place during the curing process, which leads to the generation of – Fe – O – bonds. The dehydration reaction at the time of heat curing between GO-C.R sheets and the hydroxyls that are produced on the steel surface in 3.5% NaCl is liable for the creation of – Fe – O – bonds at the interface, which results in horizontal films that block the encroachment paths in the substrate/coating interface. Also, there exists no distinguished reaction between the epoxy resin and GO-C.R sheets. However, the epoxides present in the epoxy resin forms very strong covalent bonds with unreacted hydroxyls of both the metal surface and GO-C.R sheets by ring-opening reaction [45]. This probably forms a potential barrier that hinders the ingression of corrosive ions onto the steel surface. Another mechanism for protecting steel plate by GO/C.R sheets in the epoxy matrix is the enhancement of negative charge creation on the surface of GO and GO/C.R sheets upon exposure to 3.5% NaCl solution. This probably increases the ionic resistance of epoxy matrix. This hypothesis can be evidenced by investigating the surface charges of GO and GO/C.R sheets through the measurement of zeta potential values at seawater pH of 8. It can be seen that in Fig. 15 that GO-C.R has shown more negative values than GO.

The enhancement in anti-corrosion activity occurs when there is a reduction in the intrusion of corrosion ions onto the surface of the metal substrate. A more protective film (barrier) is deposited, because of the participation of –OH groups from both the GO-C.R sheets and metal surface and ring-opening of epoxide groups present in the epoxy resin. This layer becomes even more uniform with an increase in pH of the corrosion solution, which probably limits the decline in barrier performance of the modified sample with an increase in immersion times. This could be the cause for the increase in R_{ct} and R_c values (Table 3) of GO-C.R/Epoxy sample when compared to other samples. As a result, restriction of transferring electrons(Eq. (2)) to the cathodic areas from the anodic sites may take place.

$$2H_2O + O_2 + 4e^- \rightarrow 4OH^- \quad (2)$$

The study was further extended with the intention of increasing the adhesion strength of the neat epoxy coatings via microencapsulation technique. For that motive, GO and GO-C.R encapsulated urea-formaldehyde microcapsules were synthesized via an in-situ polymerization reaction. During the reaction, urea reacts with formaldehyde and produces cross-links. These cross-links engulf GO and GO-C.R sheets as core materials, resulting in the formation of microcapsules. Fig. 6 depicts poly(urea-formaldehyde) microcapsules filled with GO and GO-C.R sheets acting as core materials. The synthesis of microcapsules takes two steps: (i) basic methylolation step where urea reacts with formaldehyde to form methylol ureas and (ii) condensation step involving the formation of urea-formaldehyde dimers, trimers, and oligomers of methylol ureas. During the process, ammonium chloride (NH_4Cl) was added, which improves the strength and sealing performance of the microcapsules. Further, the rough surface of the microcapsule could be accounted

Table 5
Adhesion indices from Peel off test.

Samples	Maximum Peel strength (*N*)	Standard deviation (σ)	Variance (*V*)
Untreated/ Epoxy	86	0.21	0.16
GO/Epoxy	92	0.23	0.19
GO-C.R/Epoxy	152	0.40	0.21
UF-GO/Epoxy	234	0.50	0.25
UF-GO-C.R/ Epoxy	290	0.55	0.30

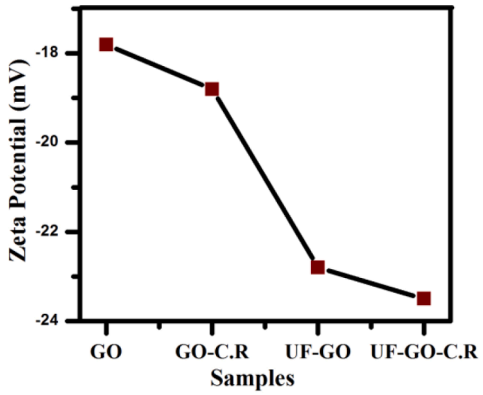

Fig. 15. Zeta potential values of GO, GO-C.R, UF-GO, UF-GO-C.R at pH 8 in 3.5 % NaCl solution.

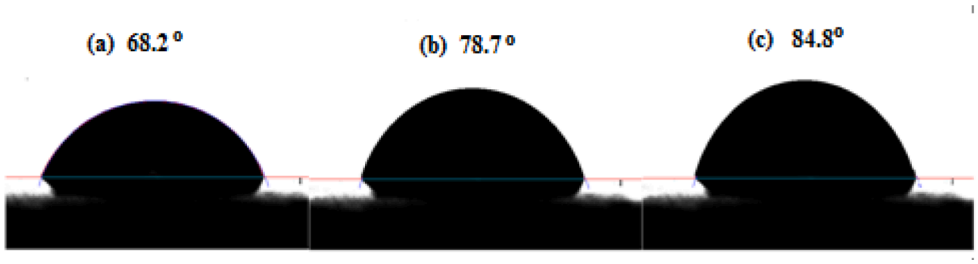

Fig. 14. Contact angle measurements on (a) Untreated/Epoxy, (b) UF-GO/ Epoxy, and (c) UF-GO-C.R/Epoxy coatings.

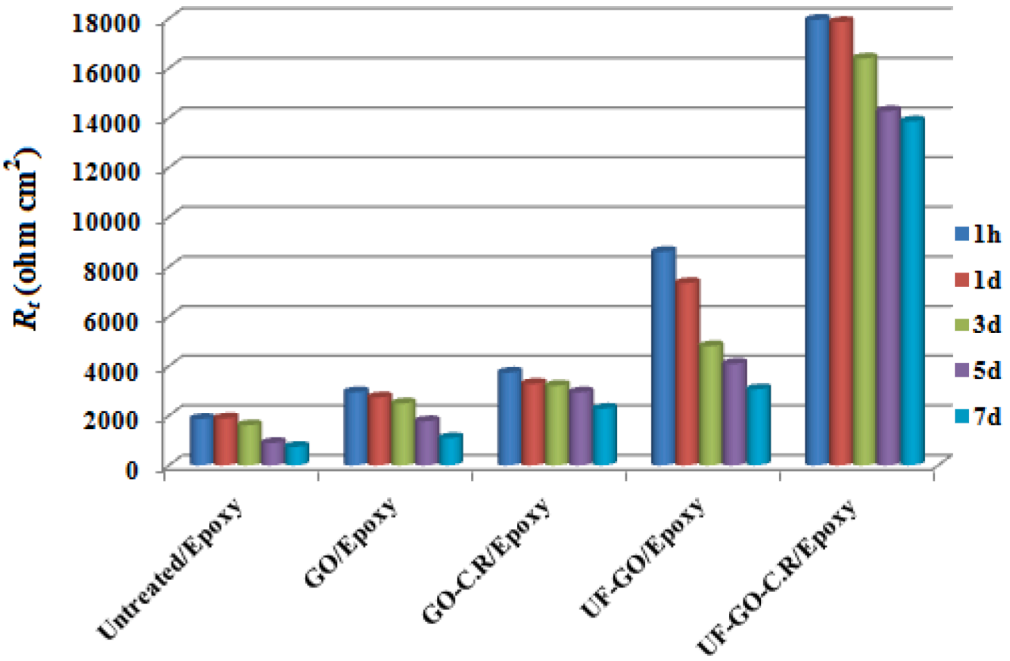

Fig. 16. Total Resistance (R_t) values for Untreated/Epoxy, GO/Epoxy, GO-C.R/Epoxy, UF-GO/Epoxy and UF-GO-C.R/Epoxy steel samples immersed in 3.5% NaCl solution.

for by the precipitation of urea-formaldehyde particles from the emulsion to an inhibitor-water interface which was driven by the active materials produced as a result of the reaction between ammonium chloride and hydroxymethylol urea. In addition, ammonium chloride decreases pH of the reaction mixture by following the equations [43]:

$$NH_4Cl + HCHO \rightarrow (CH_2)_6N_4 + HCl + H_2O \quad (3)$$

$$NH_4Cl + H_2O \rightarrow NH_4OH + HCl \quad (4)$$

Zeta potential measurements were carried out to evaluate the ionic resistance activity of the prepared microcapsules. From Fig. 15 UF-GO and UF-GO-C.R microcapsules showed even more negative values than neat GO and GO-C.R sheets, providing an improvement in the ionic resistance of UF incorporated epoxy coatings. Also, the increase in static water contact angle and decrease in surface free energy of UF-GO-C.R/Epoxy was attributed to GO-C.R encapsulated microcapsules in the neat epoxy resin showing the shift of modified epoxy coatings towards hydrophobic behavior. This behavior reduces the intrusion of corrosive ions (Cl^-, H_2O & O_2) onto the steel surface. This is achieved by the compactness and uniformity of UF-GO/GO-C.R epoxy film formed by self release of GO/GO-C.R sheets on the steel surface (Fig. 17). This homogeneous layer enhances the barrier performance of the coatings,

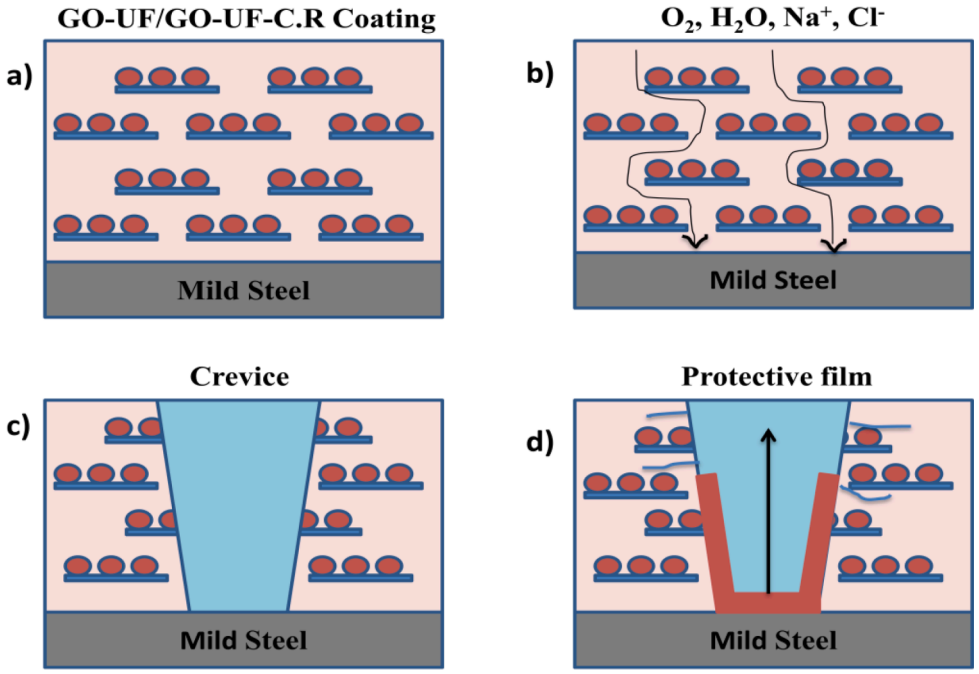

Fig. 17. Schematic representation of (a) GO-UF/GO-UF-C.R Epoxy coatings (b) influence of corrosive ions (c, d) barrier performance of GO-UF/GO-UF-C.R Epoxy coating on the metal surface via protective layer formation verses immersion in sea water.

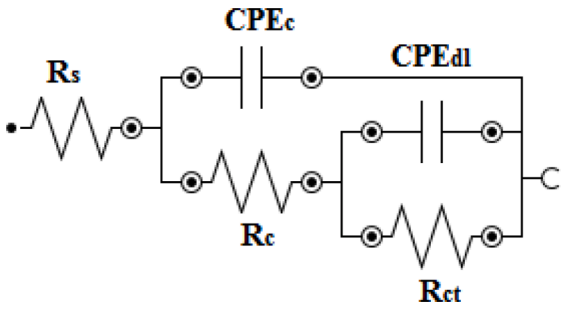

Fig. 18. The electrical circuit used for fitting EIS data.

probably by limiting the flow of corrosion electrolyte. This causes an increase in R_{ct} and R_c values (Table 3) of microcapsules incorporated coatings than other samples. The metal dissolution process could be reduced [46]. Then, coating delamination was evaluated by Peel off adhesion test to evidence the improvement in the adhesion strength. From Table 5, because of strong cohesion interactions between UF-GO-C.R sheets, the adhesion strength of the coating has been increased from 86 to 290 N. Peel strength increased with the addition of UF-GO and UF-GO-C.R into the epoxy resin. The values of σ are calculated to be more for the microcapsules incorporated epoxy coated samples compared to that of the neat epoxy sample, suggesting that these samples possess good adhesion strength between the metal substrate and modified epoxy matrix [47]. Because of the potential barrier performance of UF-GO/GO-C.R in the epoxy system and its improvement in adhesion strength, corrosion products and blisters formed around the scratch are decreased when compared to untreated/Epoxy and GO treated epoxy coatings. Further, higher $\log|Z|_{100mHz}$ values of UF-GO/GO-C.R/Epoxy coated samples show the higher adhesion strength between the modified epoxy coatings and steel substrate and long-term resistance [48] against corrosion process.

6. Conclusions

- FT-IR, FE-SEM and E-DAX tests evidenced that GO was successfully modified by phytocomponents of ***Cardiospermum halicacabum*** **L.** leaf extract through adsorption mechanism and improved dispersion in an epoxy matrix
- FT-IR, FE-SEM and TGA-DSC studies confirmed the incorporation of GO and GO-C.R sheets into urea-formaldehyde capsules via in-situ polymerization technique. Microcapsules showed enhanced corrosion resistivity when compared to neat GO and GO-C.R
- The GO-C.R loaded urea-formaldehyde microcapsules produced strong bonding with the steel surface and themselves through the creation of – Fe – O– linkages at the interface between the coating and surface of the steel substrates. These cross-links prohibited the transport of Na^+ ions to the cathodic areas.
- EIS, Salt spray test, and peel-off test showed improved corrosion protection and superior adhesion strength (290 N) for urea-formaldehyde GO-C.R microcapsules applied on the steel substrates most likely due to excellent barrier performance against the intrusion of corrosion electrolyte to the surface of the steel

Declaration of Competing Interest

The authors declare that they have no known competing financial interests or personal relationships that could have appeared to influence the work reported in this paper.

Acknowledgments

The authors gratefully thank PSGR Krishnammal College for Women for the financial support.

References

[1] A Dehghani, G Bahlakeh, B Ramezanzadeh, M. Ramezanzadeh, A combined experimental and theoretical study of green corrosion inhibition of mild steel in HCl solution by aqueous Citrullus lanatus fruit (CLF) extract, J. Mol. Liq. 279 (2019) 603–624, https://doi.org/10.1016/j.molliq.2019.02.010.
[2] Kunal Wazarkara, Deepak Patil, Ajay Rane, Dinesh Balgude, Mukesh Kathalewar, Anagha Sabnis, Microencapsulation: An Emerging Technique in Modern Coating Industry, RSC Adv. 00 (2013) 1–3, https://doi.org/10.1039/C6RA13237E.
[3] C Ho, S Huang, S Lee, Y. Chang, All Changes mark as blue Evaluation of synthesized graphene oxide as corrosion, Appl. Surf. Sci. (2017), https://doi.org/10.1016/j.apsusc.2017.10.129.
[4] L Liu, J. Xu, A study of the erosion-corrosion behavior of nano-Cr_2O_3 particles reinforced Ni-based composite alloying layer in aqueous slurry environment, Vacuum 85 (6) (2011) 687–700, https://doi.org/10.1016/j.vacuum.2010.10.009.
[5] JE Gray, B. Luan, Protective coatings on magnesium and its alloys - A critical review, J. Alloys Compd. 336 (1–2) (2002) 88–113, https://doi.org/10.1016/S0925-8388(01)01899-0.
[6] D Wang, GP. Bierwagen, Sol-gel coatings on metals for corrosion protection, Prog. Org. Coatings 64 (4) (2009) 327–338, https://doi.org/10.1016/j.porgcoat.2008.08.010.
[7] R Kumar, M Malviya, KR Ansari, H Lgaz, DS Chauhan, A. Quraishi, Functionalized graphene oxide as a new generation corrosion inhibitor for industrial pickling process : DFT and experimental approach, Mater. Chem. Phys. 236 (September 2017), 121727, https://doi.org/10.1016/j.matchemphys.2019.121727, 2019.
[8] S Arash, E Alibakhshi, G. Bahlakeh, A detailed atomic level computational and electrochemical exploration of the Juglans regia green fruit shell extract as a sustainable and highly ef fi cient green corrosion inhibitor for mild steel in 3 . 5 wt % NaCl solution, J. Mol. Liq. 284 (2019) 682–699, https://doi.org/10.1016/j.molliq.2019.04.045.
[9] MY Jiang, LK Wu, JM Hu, JQ. Zhang, Silane-incorporated epoxy coatings on aluminum alloy (AA2024). Part 1: Improved corrosion performance, Corros. Sci. 92 (2015) 118–126, https://doi.org/10.1016/j.corsci.2014.11.046.
[10] Singhbabu YN, Sivakumar B, Singh JK, Bapari H, Pramanick AK, Sahu RK. in a seawater environment using an oil-based. 2015:8035-8047. doi:10.1039/c5nr01453k.
[11] X Liu, Y Shao, Y Zhang, G Meng, T Zhang, F. Wang, Using high-temperature mechanochemistry treatment to modify iron oxide and improve the corrosion performance of epoxy coating - I. High-temperature ball milling treatment, Corros. Sci. 90 (2015) 451–462, https://doi.org/10.1016/j.corsci.2014.04.015.
[12] C Science, G Britain, P Press, T Maksimovic, MPO Box, O. Belgrade, The corrosion behaviour of epoxy-resin electrocoated steel, Corros. Sci. 33 (2) (1992) 271–279.
[13] M Sababi, H Terryn, JMC. Mol, The influence of a Zr-based conversion treatment on interfacial bonding strength and stability of epoxy coated carbon steel, Prog. Org. Coatings 105 (2017) 29–36, https://doi.org/10.1016/j.porgcoat.2016.11.016.
[14] L Chen, S Chai, K Liu, et al., Enhanced epoxy/silica composites mechanical properties by introducing graphene oxide to the interface, ACS Appl. Mater. Interfaces 4 (8) (2012) 4398–4404, https://doi.org/10.1021/am3010576.
[15] SY Yang, WN Lin, YL Huang, et al., Synergetic effects of graphene platelets and carbon nanotubes on the mechanical and thermal properties of epoxy composites, Carbon N Y 49 (3) (2011) 793–803, https://doi.org/10.1016/j.carbon.2010.10.014.
[16] N Parhizkar, T Shahrabi, B. Ramezanzadeh, Steel surface pre-treated by an advance and eco-friendly cerium oxide nanofilm modified by graphene oxide nanosheets; electrochemical and adhesion measurements, J. Alloys Compd. 747 (2018) 109–123, https://doi.org/10.1016/j.jallcom.2018.03.022.
[17] JR Potts, DR Dreyer, CW Bielawski, RS. Ruoff, Graphene-based polymer nanocomposites, Polymer (Guildf) 52 (1) (2011) 5–25, https://doi.org/10.1016/j.polymer.2010.11.042.
[18] Model G. Article in press. 2015. doi:10.1016/j.corsci.2015.11.008.
[19] Z Yu, H Di, Y Ma, et al., Fabrication of graphene oxide-alumina hybrids to reinforce the anti-corrosion performance of composite epoxy coatings, Appl. Surf. Sci. 351 (2015) 986–996, https://doi.org/10.1016/j.apsusc.2015.06.026.
[20] LC Tang, YJ Wan, D Yan, et al., The effect of graphene dispersion on the mechanical properties of graphene/epoxy composites, Carbon N Y 60 (2013) 16–27, https://doi.org/10.1016/j.carbon.2013.03.050.
[21] X Wang, W Xing, P Zhang, L Song, H Yang, Y. Hu, Covalent functionalization of graphene with organosilane and its use as a reinforcement in epoxy composites, Compos. Sci. Technol. 72 (6) (2012) 737–743, https://doi.org/10.1016/j.compscitech.2012.01.027.
[22] S Pourhashem, MR Vaezi, A Rashidi, MR. Bagherzadeh, Exploring corrosion protection properties of solvent based epoxy-graphene oxide nanocomposite coatings on mild steel, Corros. Sci. 115 (2017) 78–92, https://doi.org/10.1016/j.corsci.2016.11.008.
[23] NI Zaaba, KL Foo, U Hashim, SJ Tan, W Liu, CH. Voon, Synthesis of Graphene Oxide using Modified Hummers Method : Solvent Influence, Procedia Eng. 184 (2017) 469–477, https://doi.org/10.1016/j.proeng.2017.04.118.
[24] Di H, Yu Z, Ma Y, et al. Graphene oxide decorated with Fe 3 O 4 nanoparticles with advanced anticorrosive properties of epoxy coatings. 2016;0:1-8. doi:10.1016/j.jtice.2016.04.002.
[25] S Pourhashem, MR Vaezi, A. Rashidi, Investigating the effect of SiO2-graphene oxide hybrid as inorganic nanofiller on corrosion protection properties of epoxy coatings, Surf. Coat. Technol. (2017), https://doi.org/10.1016/j.surfcoat.2017.01.013.

[26] B Paulchamy, G Arthi, L. Bd, A Simple Approach to Stepwise Synthesis of Graphene Oxide Nanomedicine, Nanotechnology 6 (1) (2015) 1–4, https://doi.org/10.4172/2157-7439.1000253.
[27] A Habibiyan, B Ramezanzadeh, M Mahdavian, G Bahlakeh, M. Kasaeian, Rational Assembly of Mussel-Inspired Polydopamine (PDA) -Zn (II) Complex Nanospheres on Graphene Oxide Framework Tailored for Robust Self-Healing Anti, Chem. Eng. J. (2019), 123630, https://doi.org/10.1016/j.cej.2019.123630 (Ii).
[28] B Ramezanzadeh, S Niroumandrad, A Ahmadi, M Mahdavian, Mohamadzadeh Moghadam MH. Enhancement of barrier and corrosion protection performance of an epoxy coating through wet transfer of amino functionalized graphene oxide, Corros. Sci. 103 (2016) 283–304, https://doi.org/10.1016/j.corsci.2015.11.033.
[29] B Ramezanzadeh, E Ghasemi, M Mahdavian, E Changizi, Mohamadzadeh Moghadam MH. Covalently-grafted graphene oxide nanosheets to improve barrier and corrosion protection properties of polyurethane coatings, Carbon N Y 93 (2015) 555–573, https://doi.org/10.1016/j.carbon.2015.05.094.
[30] VA Online, M. Mahdavian, RSC Adv. (2016), https://doi.org/10.1039/C6RA04843A.
[31] Parhizkar N, Shahrabi T, Ramezanzadeh B. Synthesis and characterization of a unique isocyanate silane re duce d graphene oxide nanosheets ; Screening the role of multifunctional nanosheets on the adhesion and corrosion protection performance of. 2017;0:1-19. doi:10.1016/j.jtice.2017.10.033.
[32] M Mo, W Zhao, Z Chen, et al., RSC Advances performance of polyurethane composite coatings reinforced with functionalized graphene and graphene oxide nanosheets †, RSC Adv. 5 (2015) 56486–56497, https://doi.org/10.1039/C5RA10494G.
[33] K Chang, M Hsu, H Lu, M Lai, P. Liu, Room-temperature cured hydrophobic epoxy /graphene composites as corrosion inhibitor for cold-rolled steel, Carbon N Y 66 (2013) 144–153, https://doi.org/10.1016/j.carbon.2013.08.052.
[34] J Li, J Cui, J Yang, Y Ma, H Qiu, J. Yang, Progress in Organic Coatings Silanized graphene oxide reinforced organofunctional silane composite coatings for corrosion protection, Prog. Org. Coatings 99 (2016) 443–451, https://doi.org/10.1016/j.porgcoat.2016.07.008.
[35] N Palaniappan, I Cole, F Caballero-Briones, S Manickam, Justin Thomas KR, Santos D. Experimental and DFT studies on the ultrasonic energy-assisted extraction of the phytochemicals of: Catharanthus roseus as green corrosion inhibitors for mild steel in NaCl medium, RSC Adv. 10 (9) (2020) 5399–5411, https://doi.org/10.1039/c9ra08971c.
[36] MS Eluyemi, MA Eleruja, AV. Adedeji, et al., Synthesis and Characterization of Graphene Oxide and Reduced Graphene Oxide Thin Films Deposited by Spray Pyrolysis Method, Graphene 05 (03) (2016) 143–154, https://doi.org/10.4236/graphene.2016.53012.
[37] S Zhou, Y Wu, W Zhao, et al., Designing reduced graphene oxide/zinc rich epoxy composite coatings for improving the anticorrosion performance of carbon steel substrate, Mater. Des. (2019) 107694, https://doi.org/10.1016/j.matdes.2019.107694.
[38] Y Hayatgheib, B Ramezanzadeh, P Kardar, M. Mahdavian, A comparative study on fabrication of a highly effective corrosion protective system based on graphene oxide-polyaniline nanofibers/epoxy composite, Corros. Sci. 133 (January) (2018) 358–373, https://doi.org/10.1016/j.corsci.2018.01.046.
[39] Bahlakeh G, Ramezanzadeh B, Ramezanzadeh M. Cerium Oxide Nanoparticles Influences on the Binding and Corrosion Protection Characteristics of a Melamine-Cured Polyester Resin on Mild Steel: An Experimental, Density Functional Theory and Molecular Dynamics Simulation Studies. Elsevier Ltd; 2017. doi:10.1016/j.corsci.2017.01.021.
[40] S Liu, L Gu, H Zhao, J Chen, H. Yu, Corrosion Resistance of Graphene-Reinforced Waterborne Epoxy Coatings, J. Mater. Sci. Technol. 32 (5) (2016) 425–431, https://doi.org/10.1016/j.jmst.2015.12.017.
[41] Online VA, Liu S, Yu H. RSC Advances. 2015. doi:10.1039/C5RA08591H.
[42] AS HICYILMAZ, AC BEDELOGLU, In Situ Graphene Oxide Reinforced Poly (Urea - Formaldehyde) Microencapsulation of Epoxy, Mater. Sci. Res. India 16 (1) (2019) 07–13, https://doi.org/10.13005/msri/160103.
[43] M Fadil, DS Chauhan, MA. Quraishi, Smart Coating Based on Urea-Formaldehyde Microcapsules Loaded with Benzotriazole for Corrosion Protection of Mild Steel in 3.5 % NaCl, Russ. J. Appl. Chem. 91 (10) (2018) 1721–1728, https://doi.org/10.1134/S107042721810021X.
[44] A. Press, A Reformulation of the Equation of State for Interfacial Tensions 137 (1) (1990) 1–4.
[45] AH Zheng, Y Shao, Wang Y. Highlights : *Eval Program Plann* (2017), https://doi.org/10.1016/j.corsci.2017.04.019.
[46] B Nikpour, B Ramezanzadeh, G Bahlakeh, M. Mahdavian, Synthesis of graphene oxide nanosheets functionalized by green corrosion inhibitive compounds to fabricate a protective system, Corros. Sci. (January) (2017) 0–1, https://doi.org/10.1016/j.corsci.2017.08.029.
[47] Vaca-cortés E, Lorenzo MA, Jirsa JO, Wheat HG, Carrasquillo RL. Adhesion testing of epoxy coating. 1998;(1265).
[48] N Parhizkar, T Shahrabi, B. Ramezanzadeh, A New Approach for Enhancement of the Corrosion Protection Properties and Interfacial Adhesion Bonds between the Epoxy Coating and Steel Substrate through Surface Treatment by Covalently Modified Amino Functionalized Graphene Oxide Film, Eval. Program. Plann. (2017), https://doi.org/10.1016/j.corsci.2017.04.011.
[49] Syahfitri TWW, Yulizar Y, Gunlazuardi J, Apriandanu DOB. TiO2/Co3O4nanocomposite: Synthesis via Catharanthus roseus (L.) G. Don leaf extract, characterization and its photocatalytic activity for malachite green degradation, *IOP Conf .ser. Mater. Sci. Eng.* 2020, 902(1), doi:10.1088/1757-899X/902/1/012003.